JOURNAL OF AIRCRAFT
Vol. 50, No. 1, January–February 2013

Predicting Limit Cycle Oscillation in an Aeroelastic System Using Nonlinear Normal Modes

Christopher W. Emory* and Mayuresh J. Patil†
Virginia Polytechnic Institute and State University, Blacksburg, Virginia 24060

DOI: 10.2514/1.C031668

This paper demonstrates the use of nonlinear normal modes to predict limit cycle oscillation in a pitch-plunge airfoil with cubically nonlinear pitch stiffness. Aeroelastic systems with quasi-steady and unsteady aerodynamics are analyzed with nonlinear normal modes. An alternative derivation of nonlinear normal modes using first-order form is offered for systems that cannot fit the standard second-order form. The effect of the master coordinate chosen to construct the nonlinear normal modes is examined and found to have a significant impact on the accuracy of the results. Based on the results herein the nonlinear normal mode method is found to be a viable approach to studying and predicting limit cycle oscillation in aeroelastic systems. Furthermore, a master coordinate based on the the linear flutter mode was found to lead to the best results.

I. Introduction

A NUMBER of modern aircraft, such as the F-16 and F-18, have experienced a phenomenon termed as limit cycle oscillation (LCO) in which the wing behaves similarly to classic flutter but does not diverge. One or more nonlinearities, such as geometric, aerodynamic, stiffness, or structural damping, in the system act to limit the amplitude of the motion. In the case of the F-16, the occurrence of LCO can make it difficult or impossible for the aircrew to perform necessary tasks. If the amplitude is large enough the motion can damage the aircraft or stores attached to the wings [1].

Flutter has typically been modeled with linear analysis. Because LCO is by its very nature nonlinear, these linear models are not capable of predicting all aspects of LCO. Linear flutter analysis has been demonstrated to be adequate to predict the frequency and modal composition, but it is incapable of identifying the onset velocity or the amplitude [2]. This inability to fully predict the LCO creates the need for extensive flight testing. For an aircraft like the F-16, the number of under-wing store configurations has been increasing and flight testing costs are continually rising [3]. Denegri et al. [2,3] identifies the need for a nonlinear flutter analysis method capable of predicting all the aspects of LCO behavior.

Various computational and experimental approaches have been pursued to aid in the development of a model capable of capturing the physics involved in LCO. Most approaches simply are not practical for modeling a real-world case like the F-16 due to the large amount of computation necessary. One of the most promising modeling approaches, harmonic balance, has been applied to a few F-16 test cases with somewhat favorable results [4].

The classic pitch-plunge airfoil with some added nonlinearities is a common first step in attempting to model LCO. The first nonlinear investigation of this model was conducted by Woolston et al. [5] through the use of an analog computer. Lee and LeBlanc [6] analyzed a cubically nonlinear model by time marching the nonlinear differential equations with Houbolt's [7] implicit finite-difference method. Houbolt's time-marching scheme was later used in many other papers. An airfoil with bilinear and cubic nonlinearities in pitch was investigated by Price et al. [8]. They used Wagner's function for the aerodynamics and the nonlinear differential equations were integrated with the finite-difference method of Houbolt [7]. The equations were also solved with the harmonic-balance method which was originally derived by Krylov and Bogoliubov [9]. Lee et al. [10] introduced four new aerodynamic variables to eliminate the aerodynamic lag integrals in the aeroelastic equations of motions. Earlier work had solved integrals at each time step for the unsteady aerodynamics. With the elimination of the integrals, the system could be written in terms of eight first-order ordinary differential equations in the time domain, making analytical analysis of the equations possible. Center manifold theory was applied to the nonlinear airfoil by Liu et al. [11]. The pitch-plunge airfoil equations were formulated in the eight first-order differential equation form. The center manifold theory was then applied to reduce the order of the system from eight to two states.

The goal of this work is to take a step toward a new, practical method of nonlinear analysis to predict LCO that offers insight into the physics underlying the LCO phenomena. Furthermore, the analysis methodology should be extendable to complex real world problems in the future. The method of nonlinear normal modes (NNM) is explored here for LCO prediction. The NNM model can reduce the system to either a single second-order, single degree-of-freedom, nonlinear, differential equation or a pair of coupled first-order, nonlinear, differential equations while maintaining dominant nonlinearity and the effect of all degrees of freedom desired in the model. Only having to solve a system with a single degree of freedom could save considerable computational time. The method should also offer some unique information about the physical modeshapes involved in LCO motion.

There are two main definitions of NNMs in literature. The first definition, developed by Rosenberg, defines the NNMs as synchronous oscillation requiring all degrees of freedom to pass through zero at the same time [12]. This definition obviously limits itself to conservative systems and is not applicable to the nonconservative aeroelastic pitch-plunge airfoil system. The second NNM definiton, used in this paper, was developed by Shaw and Pierre [13] by extending the linear system concept of normal modes of vibration to general nonlinear systems. Drawing inspiration from the center manifold reduction technique, they constructed invariant manifolds which represent normal modes of motion for nonlinear systems with finite degrees of freedom. Their initial paper constructed the manifold with an approximate asymptotic approach restricting it to weakly nonlinear systems. A number of extensions and improvements have since been made to the method of nonlinear normal modes. Shaw and Pierre [14] reformulated the method for continuous systems. The original single mode manifolds were not capable of modeling internal resonances present in the system. Pesheck et al. [15] developed

Presented as Paper 2011-1742 at the Structural Dynamics and Materials 2011, Denver, CO, 4–7 April 2011; received 18 September 2011; revision received 15 June 2012; accepted for publication 26 June 2012; published online 2 January 2013.

*Graduate Student, Aerospace and Ocean Engineering; currently Flutter Engineer, Air Force SEEK Eagle Office, Eglin Air Force Base, FL. Member AIAA.

†Associate Professor, Aerospace and Ocean Engineering. Associate Fellow AIAA.

multimode manifolds that made it possible to include coupling between modes due to internal resonance in a single nonlinear normal mode. A Galerkin-based approach to formulating the manifolds was introduced by Pesheck et al. [16], which allowed the user to prescribe a domain and order of accuracy of the nonlinear normal mode. All of the nonlinear normal modes mentioned so far assumed the system was unforced. Jiang et al. [17] incorporated the ability to include a harmonic excitation into the method.

This paper specifically deals with an asymptotic formulation of nonlinear normal modes used to study a nonlinear version of the classic pitch-plunge airfoil model. Both quasi-steady and unsteady aerodynamic models are considered. The effect of the choice of the master coordinate is also examined. All the results are compared to a fourth-order Runge-Kutta solution of the original equations of motion.

II. Theory

A. Nonlinear Pitch-Plunge Airfoil

The aeroelastic model considered in this paper is a nonlinear variation of the classic pitch-plunge airfoil as seen in Fig. 1. The nondimensional equations of motion for the pitch-plunge airfoil are

$$\ddot{\bar{h}} + x_\alpha \ddot{\alpha} + \bar{\omega}^2 \bar{h} = -\bar{L} \quad x_\alpha \ddot{\bar{h}} + r_\alpha^2 \ddot{\alpha} + r_\alpha^2 (1 + G_\alpha \alpha^2)\alpha = \bar{M} \tag{1}$$

These equations only differ from the classic equations that appear in Bisplinghoff et al. [18] by the dimensionless, nonlinear stiffness term G_α. The variables in Eq. (1) and Fig. 1 are as follows: $\bar{h}$ is the nondimensional plunge, which is the plunge displacement h divided by the semichord b, α is the pitch, I_α is the pitch inertia, m is the mass, x_α is the dimensionless static imbalance, $K_\alpha[\alpha] = k_\alpha(1 + G_\alpha \alpha^2)$, $\bar{\omega}$ is the plunge-pitch natural frequency ratio $\frac{\omega_h}{\omega_\alpha}$ where $\omega_h = \sqrt{\frac{K_h}{m}}$ and $\omega_\alpha = \sqrt{\frac{k_\alpha}{I_\alpha}}$, r_α is the dimensionless radius of gyration $\sqrt{\frac{I_\alpha}{mb^2}}$, and an overdot represents a time derivative. The nondimensional lift and moment appear as $\bar{L}$ and $\bar{M}$.

The aerodynamic lift and moment were modeled with Theodorsen's lift and moment equations [19].

$$\begin{aligned}
\bar{L} &= \frac{1}{\mu}\left\{\ddot{\bar{h}} + \bar{U}\dot{\alpha} - a\ddot{\alpha} + 2\bar{U}C[k]\left(\dot{\bar{h}} + \bar{U}\alpha + \left(\frac{1}{2} - a\right)\dot{\alpha}\right)\right\} \\
\bar{M} &= \frac{1}{\mu}\left\{a\ddot{\bar{h}} - \left(\frac{1}{2} - a\right)\bar{U}\dot{\alpha} - \left(\frac{1}{8} + a^2\right)\ddot{\alpha}\right\} \\
&\quad + 2\bar{U}\frac{1}{\mu}\left(\frac{1}{2} + a\right)C[k]\left\{\dot{\bar{h}} + \bar{U}\alpha + \left(\frac{1}{2} - a\right)\dot{\alpha}\right\}
\end{aligned} \tag{2}$$

In these equations $\bar{U}$ is the dimensionless freestream velocity $\frac{V_\infty}{b\omega_\alpha}$, a is the elastic axis location, $C[k]$ is Theodorsen's function, and μ is the density ratio $\frac{m}{\pi b^2 \rho}$.

B. Aerodynamic Models

1. Quasi-Steady Aerodynamics

For quasi-steady aerodynamics $C[k]$ is set to unity. The resulting quasi-steady aeroelastic system is directly compatible with the NNM method and no further manipulation is required.

2. Unsteady Aerodynamics

The pitch-plunge airfoil was also considered with unsteady aerodynamics. The same equations from the quasi-steady model, Eqs. (1) and (2), are used except $C[k]$ is not set to unity. For unsteady aerodynamics, $C[k]$ is in the frequency domain, which is not compatible with the NNM method that requires analytic, time-domain equations. To facilitate the nonlinear normal mode method the lift and moment were rewritten as

$$\begin{aligned}
\bar{L} &= \frac{1}{\mu}(\ddot{\bar{h}} + \bar{U}\dot{\alpha} - a\ddot{\alpha} + 2\bar{U}L_c) \\
\bar{M} &= \frac{1}{\mu}\left[a\ddot{\bar{h}} - \left(\frac{1}{2} - a\right)\bar{U}\dot{\alpha} - \left(\frac{1}{8} + a^2\right)\ddot{\alpha}\right] + 2\bar{U}\frac{1}{\mu}\left(\frac{1}{2} + a\right)L_c \\
L_c &= C[k]\left[\dot{\bar{h}} + \bar{U}\alpha + \left(\frac{1}{2} - a\right)\dot{\alpha}\right]
\end{aligned} \tag{3}$$

Venkatesan and Freidmann [20] developed approximate transfer functions representing Theodorsen's function through the use of Bode plots. Using two zeros and poles, Theodorsen's function can be written as

$$C[k] = \frac{0.5(ik + 0.135)(ik + 0.651)}{(ik + 0.0965)(ik + 0.4555)} \tag{4}$$

The paper showed very good agreement between the transfer function and the exact Theodorsen's equations.

To model L_c the transfer function was nondimensionalized and then converted to a state-space model with two states. The state-space model can be written as

$$\begin{aligned}
\begin{Bmatrix} \dot{x}_3 \\ \dot{x}_4 \end{Bmatrix} &= \bar{U}\begin{bmatrix} -0.0965 & 0.08676 \\ 0 & -0.4555 \end{bmatrix}\begin{Bmatrix} x_3 \\ x_4 \end{Bmatrix} \\
&\quad + \sqrt{\bar{U}}\begin{bmatrix} 0.09811 \\ 0.2211 \end{bmatrix}\left(\dot{\bar{h}} + \bar{U}\alpha + \left(\frac{1}{2} - a\right)\dot{\alpha}\right) \\
L_c &= \sqrt{\bar{U}}[0.1962 \quad 0.4422]\begin{Bmatrix} x_3 \\ x_4 \end{Bmatrix} \\
&\quad + 0.5\left(\dot{\bar{h}} + \bar{U}\alpha + \left(\frac{1}{2} - a\right)\dot{\alpha}\right)
\end{aligned} \tag{5}$$

The aerodynamic states start at x_3 because x_1 and x_2 are reserved for the modal degrees of freedom of the pitch-plunge airfoil. This state space aerodynamic model was then incorporated into the pitch-plunge airfoil system of two coupled, second-order differential equations to

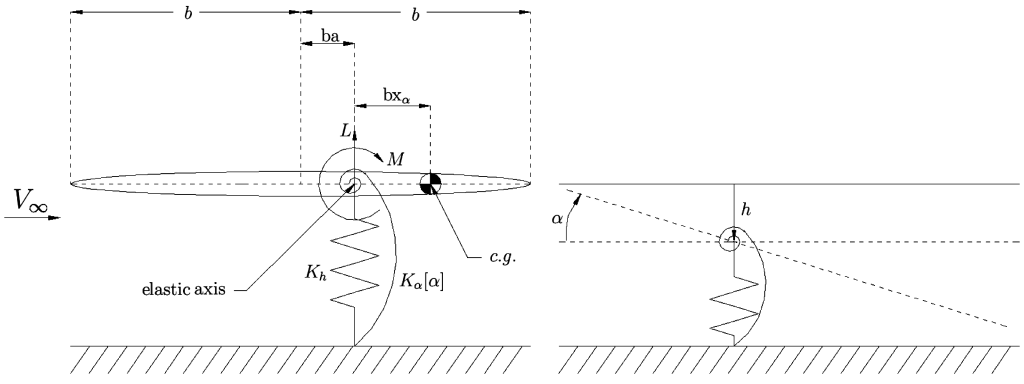

Fig. 1 Pitch-plunge airfoil model.

create a system of four equations with two second-order and two first-order differential equations. The full aeroelastic system is

$$\ddot{x}_1 + x_\alpha \ddot{x}_2 + \bar{\omega}^2(1 + G_h x_1^2)x_1 = -\bar{L}$$
$$x_\alpha \ddot{x}_1 + r_\alpha^2 \ddot{x}_2 + r_\alpha^2(1 + G_\alpha x_2^2)x_2 = \bar{M}$$
$$\dot{x}_3 = \bar{U}(-0.0965x_3 + 0.08676x_4) + 0.09811\sqrt{\bar{U}}\left(\dot{x}_1 + \bar{U}x_2 + \left(\frac{1}{2} - a\right)\dot{x}_2\right)$$
$$\dot{x}_4 = -0.4555\bar{u}x_4 + 0.2211\sqrt{\bar{U}}\left(\dot{x}_1 + \bar{U}x_2 + \left(\frac{1}{2} - a\right)\dot{x}_2\right) \tag{6}$$

where

$$\bar{L} = \frac{1}{\mu}\left(\ddot{x}_1 + \bar{U}\dot{x}_2 - a\ddot{x}_2 + 2\bar{U}\left(\sqrt{\bar{U}}(0.1962x_3 + 0.4422x_4) + 0.5\left(\dot{x}_1 + \bar{U}x_2 + \left(\frac{1}{2} - a\right)\dot{x}_2\right)\right)\right)$$
$$\bar{M} = \frac{1}{\mu}\left(a\ddot{x}_1 - \left(\frac{1}{2} - a\right)\bar{U}\dot{x}_2 - \left(\frac{1}{8} + a^2\right)\ddot{x}_2\right) + 2\bar{U}\frac{1}{\mu}\left(\frac{1}{2} + a\right) \times \left(\sqrt{\bar{U}}(0.1962x_3 + 0.4422x_4) + 0.5\left(\dot{x}_1 + \bar{U}x_2 + \left(\frac{1}{2} - a\right)\dot{x}_2\right)\right) \tag{7}$$

C. Nonlinear Normal Modes: Asymptotic Formulation

1. Nonlinear Normal Modes Standard Derivation

This section mostly follows the derivation of nonlinear normal modes by Shaw and Pierre [13]. A few changes in notation and description have been made to aid in a quick understanding of the method.

The derivation of nonlinear normal modes begins with an original system of N coupled, second-order differential equations. They must be written in the form of Eq. (8) or must be transformed to this form.

$$\ddot{x}_i = f_i(x_1, x_2, \ldots, x_N, \dot{x}_1, \dot{x}_2, \ldots, \dot{x}_N) \tag{8}$$

The N second-order equations are then transformed to $2N$ first-order pairs of differential equations.

$$\dot{x}_i = y_i$$
$$\dot{y}_i = f_i(x_1, x_2, \ldots, x_N, y_1, y_2, \ldots, y_N) \tag{9}$$

One of the x_i-y_i coordinate pairs now must be chosen as the master coordinate on which the nonlinear normal modes are based. Pair one is chosen for convenience of notation, but any of the pairs can be chosen.

$$x_1 = u$$
$$y_1 = v \tag{10}$$

The modal degrees of freedom are denoted here as u and v. The remaining system degrees of freedom are slaved to the master modal coordinate by a rule for modal motion.

$$x_i = X_i(u, v) \qquad i \neq 1$$
$$y_i = Y_i(u, v) \qquad i \neq 1 \tag{11}$$

For the rest of this derivation, the use of i does not include the value of one, which is reserved for the master coordinate. To create an asymptotic approximation of the nonlinear normal modes, $X_i(u, v)$ and $Y_i(u, v)$ are considered to be a Taylor series expansions in two variables to the desired order of the approximation.

$$X_i(u, v) = a_{1i}u + a_{2i}v + a_{3i}u^2 + a_{4i}uv + a_{5i}v^2 + \ldots$$
$$Y_i(u, v) = b_{1i}u + b_{2i}v + b_{3i}u^2 + b_{4i}uv + b_{5i}v^2 + \ldots \tag{12}$$

The a's and b's are unknown coefficients.

The first step in solving for the unknown coefficients is to take the derivative of Eq. (11).

$$\dot{x}_i = \frac{\partial X_i}{\partial u}\dot{u} + \frac{\partial X_i}{\partial v}\dot{v}$$
$$\dot{y}_i = \frac{\partial Y_i}{\partial u}\dot{u} + \frac{\partial Y_i}{\partial v}\dot{v} \tag{13}$$

The equations of motion, Eq. (9), are used to substitute for $\dot{x}_i$ and $\dot{y}_i$.

$$y_i = \frac{\partial X_i}{\partial u}\dot{u} + \frac{\partial X_i}{\partial v}\dot{v}$$
$$f_i(x_1, x_2, \ldots, x_N, y_1, y_2, \ldots, y_N) = \frac{\partial Y_i}{\partial u}\dot{u} + \frac{\partial Y_i}{\partial v}\dot{v} \tag{14}$$

Since $\dot{u} = \dot{x}_1 = y_1 = v$ and $\dot{v} = \dot{y}_1 = f_1(x_1, \ldots, x_N, y_1, \ldots, y_N)$ Eq. (14) can be rewritten as

$$y_i = \frac{\partial X_i}{\partial u}v + \frac{\partial X_i}{\partial v}f_1(x_1, x_2, \ldots, x_N, y_1, y_2, \ldots, y_N)$$
$$f_i(x_1, x_2, \ldots, x_N, y_1, y_2, \ldots, y_N) = \frac{\partial Y_i}{\partial u}v + \frac{\partial Y_i}{\partial v}f_1(x_1, x_2, \ldots, x_N, y_1, y_2, \ldots, y_N) \tag{15}$$

The remaining x_1's and y_1's are replaced by u and v Eq. (10) and the x_i's and y_i's are replaced by $X_i(u, v)$ and $Y_i(u, v)$ Eq. (11).

$$Y_i(u, v) = \frac{\partial X_i}{\partial u}v + \frac{\partial X_i}{\partial v}f_1(u, X_2(u, v), \ldots, X_N(u, v), v, Y_2(u, v), \ldots, Y_N(u, v))$$
$$f_i(u, X_2(u, v), \ldots, X_N(u, v), v, Y_2(u, v), \ldots, Y_N(u, v)) = \frac{\partial Y_i}{\partial u}v + \frac{\partial Y_i}{\partial v}f_1(u, X_2(u, v), \ldots, X_N(u, v), v, Y_2(u, v), \ldots, Y_N(u, v)) \tag{16}$$

These $2N - 2$ equations, Eq. (16), are polynomials in u and v with coefficients composed of combinations of the unknown a_{ji} and b_{ji} coefficients from Eq. (12). The $2N - 2$ system of equations is of the form

$$\sum_{k=0}^{z \cdot o}\sum_{l=0}^{(z \cdot o)-k} C_{kl}[a_{ji}, b_{ji}]u^k v^l = 0, \qquad C_{00} = 0 \tag{17}$$

In this equation, z is the order of the nonlinear modal approximation and o is the order of the nonlinearities in the system. In the asymptotic solution, the residual equations are truncated at the order of the modal approximation.

$$\sum_{k=0}^{z}\sum_{l=0}^{z-k} C_{kl}[a_{ji}, b_{ji}]u^k v^l + H.O.T. = 0, \qquad C_{00} = 0 \tag{18}$$

Now each C_{kl} can be set equal to zero to create a system of equations in a_{ji} and b_{ji}. The system is a set of nonlinear equations; however, they can be divided into subsets based on the value of $(k + l)$ and solved sequentially. The terms where $(k + l) = 1$ are coefficients of linear u and v terms in the residual equations, $(k + l) = 2$ are quadratic coefficients, etc. Now only the first set where $(k + l) = 1$ will be a nonlinear system. The solution from the first system can be substituted into the following systems, and they become systems of linear equations. Additionally, the solution for the first nonlinear system of the equations for the linear coefficients can be represented as a modal solution to the linearized equations of motion. As such, they can be found with an eigenvalue solution technique. This results in only needing an eigenvalue solution and a solution to a series of linear systems to solve for the unknown nonlinear normal-mode coefficients.

With the solution to the unknown coefficients, the modal rules Eqs. (11) and (12) can be inserted into the equations of motion of the master coordinates. Each set of a and b coefficients create a different nonlinear normal mode. The modal form of the equation will appear as

$$\dot{u} = v$$
$$\dot{v} = f_1(u, X_2(u,v), \ldots, X_N(u,v), v, Y_2(u,v), \ldots, Y_N(u,v)) \quad (19)$$

or in second-order form

$$\ddot{u} = f_1(u, X_2(u,\dot{u}), \ldots, X_N(u,\dot{u}), \dot{u}, Y_2(u,\dot{u}), \ldots, Y_N(u,\dot{u})) \quad (20)$$

This equation can then be used to find the systems behavior in that mode. The modal motion found can be converted back into physical coordinates by using Eqs. (10) and (11).

2. Nonlinear Normal Modes—Alternative First-Order Derivation

The use of unsteady aerodynamics with the pitch-plunge airfoil creates a system with a mixture of first- and second-order differential equations that does not match the form required in Eq. (8). This system can easily be transformed into a system of first-order differential equations. Additionally, part of this work studied the effect different master coordinates had on the accuracy of the resultant mode. One of the master coordinates studied was the linear flutter mode at the velocity of interest. When writing the nonlinear system in terms of linear flutter mode, the system could not be formed as required in the standard NNM derivation. The resultant system was a set of coupled, nonlinear first-order equations. To deal with these two first-order systems, this derivation starts with a system of the form

$$\dot{x}_i = f_i(x_1, x_2, \ldots, x_N) \quad (21)$$

Just as before, master coordinates are chosen, but here two first-order states are needed which may or may not be related. The two master coordinates are denoted as x_1 and x_2 for convenience, but any pair can be chosen. The remaining coordinates are slaved by an asymptotic expansion.

$$x_1 = u$$
$$x_2 = v \quad (22)$$

$$x_i = X_i(u,v) = a_{1i}u + a_{2i}v + a_{3i}u^2 + a_{4i}uv + a_{5i}v^2 + \ldots \quad i \neq 1,2 \quad (23)$$

Then, invoking a process very similar to the original derivation, the following system of equations is obtained:

$$f_i(u, v, X_3(u,v), \ldots, X_N(u,v)) - \left(\frac{\partial X_i(u,v)}{\partial u} f_1(u, v, X_3(u,v), \ldots, X_N(u,v)) + \frac{\partial X_i(u,v)}{\partial v} f_2(u, v, X_3(u,v), \ldots, X_N(u,v))\right) = 0 \quad i \neq 1,2 \quad (24)$$

The unknown coefficients can be found from these equations in a fashion identical to the standard derivation.

III. Results

A. Pitch-Plunge Airfoil Data

The pitch-plunge airfoil with quasi-steady aerodynamics and a nonlinear pitch stiffness was the first aeroelastic system on which the NNM method was attempted. It was also used for studies on master-coordinate selection.

For the test cases presented, the following constants were used in Eq. (1): $\mu = 11.0$, $a = -0.35$, $x_\alpha = 0.2$, $r_\alpha = 0.5$, $\bar{\omega} = 0.5$, and $G_\alpha = 0.5$. This model has a dimensionless linear flutter speed V_f of 0.807 and linear flutter frequency of 0.1598 Hz. Other cases were tested, but the results were very nearly the same and only confirmed the conclusions reached with the model above.

B. Results with Quasi-Steady Aerodynamics

Because the system in Eq. (1) is not in the form needed for the NNM method, it must first be transformed. The simplest route is to multiply by the inverse of the mass matrix so the plunge degree of freedom can be used as the master coordinate. At each freestream velocity of interest, the standard derivation of the asymptotic NNMs was followed. The final result is two uncoupled modal equations. Below is an example of this result for a nondimensional velocity of 1.05 times the linear flutter velocity. The LCO NNM modal equation is

$$\begin{aligned}\ddot{u} = u(&-1.000 - 4.37u^2 - 9.44\dot{u}^2 - 26.5u^4 - 62.7u^2\dot{u}^2 - 7.45\dot{u}^4 \\ &- 192.1u^6 - 272u^4\dot{u}^2 + 155.2u^2\dot{u}^4 + 192.8\dot{u}^6 \\ &- 465u^8 - 1288u^6\dot{u}^2 - 1373u^4\dot{u}^4 - 900u^2\dot{u}^6 - 331\dot{u}^8) \\ &+ \dot{u}(0.00462 - 2.86u^2 + 0.312\dot{u}^2 - 68.5u^4 - 44.3u^2\dot{u}^2 \\ &+ 25.5\dot{u}^4 - 206u^6 - 231u^4\dot{u}^2 - 76.0u^2\dot{u}^4 - 69.3\dot{u}^6 \\ &+ 207u^8 + 1091u^6\dot{u}^2 + 1475u^4\dot{u}^4 + 636u^2\dot{u}^6 + 62.9\dot{u}^8) \quad (25)\end{aligned}$$

Here u is the master, modal degree of freedom as described in Eq. (20). In this particular case, because the plunge degree of freedom was selected as the master coordinate u is equal to h. This can be a particularly useful trait if one degree of freedom or mode is of primary interest. In Eq. (25), the destabilizing linear damping term ($0.00462\dot{u}$) is apparent in this LCO modal equation. Based on the second damping term ($-2.86u^2\dot{u}$), it is clear that small but finite motion has a stabilizing effect. The third term ($+0.312\dot{u}^3$) is of the same order as the second term, but for a flutter frequency around 0.1598 is much smaller value than the second term. Thus, one can infer that even though the mode is linearly unstable, the primary nonlinear terms are stabilizing. The second NNM modal equation is a damped oscillator as would be expected.

$$\begin{aligned}\ddot{u} = u(&-0.236 + 0.00179u^2 - 0.01472\dot{u}^2 - 0.000434u^4 \\ &- 0.00874u^2\dot{u}^2 - 0.0316\dot{u}^4 + 0.00001555u^6 + 0.000555u^4\dot{u}^2 \\ &+ 0.00549u^2\dot{u}^4 + 0.01460\dot{u}^6 - 1.855\times10^{-7}u^8 \\ &- 9.72\times10^{-6}u^6\dot{u}^2 - 0.0001631u^4\dot{u}^4 - 0.001066u^2\dot{u}^6 \\ &- 0.00224\dot{u}^8) + \dot{u}(-0.207 + 0.00738u^2 - 0.00469\dot{u}^2 \\ &- 0.00224u^4 - 0.0239u^2\dot{u}^2 - 0.01516\dot{u}^4 + 0.0000965u^6 \\ &+ 0.00207u^4\dot{u}^2 + 0.01151u^2\dot{u}^4 + 0.00738\dot{u}^6 \\ &- 1.347\times10^{-6}u^8 - 0.0000443u^6\dot{u}^2 - 0.000483u^4\dot{u}^4 \\ &- 0.001865u^2\dot{u}^6 - 0.001197\dot{u}^8) \quad (26)\end{aligned}$$

The stabilizing linear damping is easily visible in this damped modal equation.

In addition to calculating the NNM, a linear normal mode (LNM) was also calculated for comparison. The LNM is found using the same process as the NNM except the modal approximation equations [Eq. (12)] only contain linear terms. This significantly reduces the computational effort and results in an approximation that retains the nonlinearity in a particular mode, but neglects the nonlinear coupling between modes. The LCO mode calculated with the LNM is

$$\begin{aligned}\ddot{u} = u(&-1.000 - 1.215u^2 - 6.83\dot{u}^2) \\ &+ \dot{u}(0.00462 - 4.99u^2 - 3.12\dot{u}^2) \quad (27)\end{aligned}$$

The damped modal equation using LNM is

$$\ddot{u} = u(-0.236 + 0.00404u^2 + 0.0228\dot{u}^2) + \dot{u}(-0.207 + 0.01661u^2 + 0.01039\dot{u}^2) \tag{28}$$

The stabilizing and destabilizing linear damping terms can also be seen in these LNM equations. Comparing these two sets of equations, it is obvious that the NNM equations capture significantly more nonlinear coupling terms than the LNM equations.

The Runge-Kutta simulation of the NNM modal equation for LCO is compared to a simulation of the original equation of motion and the LNM equation of motion for LCO. All the simulations, including the exact solution, are based on a modal initial condition corresponding to the LCO NNM. Figure 2 shows the growth of LCO motion from an initial condition and Fig. 3 shows the final converged LCO in phase space. As can be seen in the time-history and phase-space plots, the NNM does a very good job of modeling LCO motion and growth. If plotted on the same graph, the NNM and the exact time histories are nearly indistinguishable. The NNM is obviously much better than the LNM. The reason the LNM equation does not do well is obvious when Eqs. (25) and (27) are compared. The LNM equation is missing a vast majority of the nonlinear terms and does not capture accurately the ones it does contain.

Figure 4 shows a time history for the damped modes. Only a single line is plotted because both the NNM and the LNM give a nearly exact solution for the damped mode's decay. All of this motion occurs in the linear amplitude range and because the linear parts of both solutions are exact, a nearly exact solution is produced. These are not exact solutions because the nonlinear terms still exist and are inexact

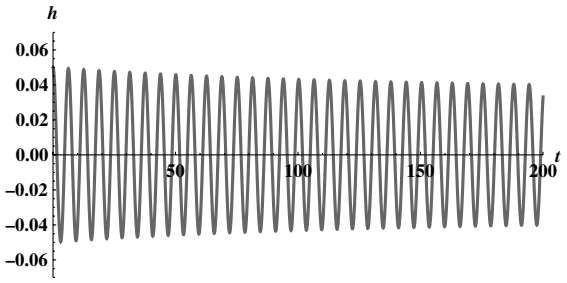

a) LNM

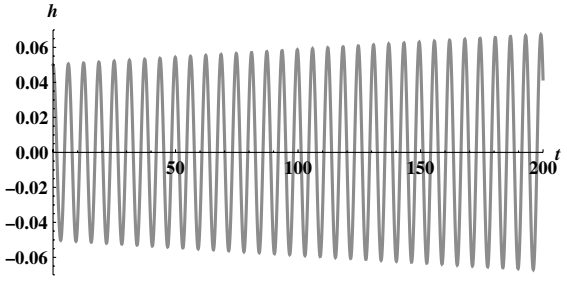

b) NNM

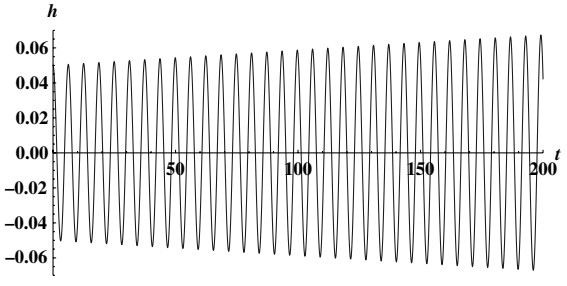

c) Exact

Fig. 2 Plunge time-history plots of quasi-steady airfoil at $1.05V_f$.

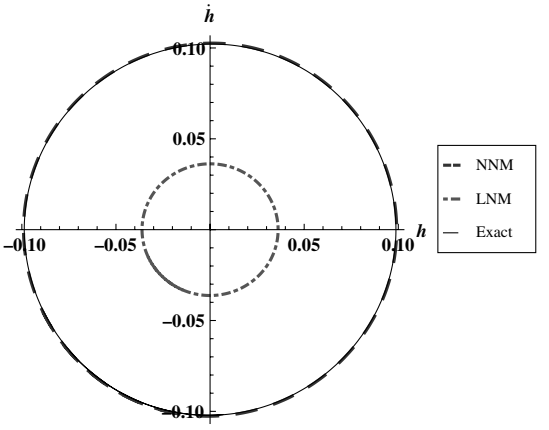

a) Plunge

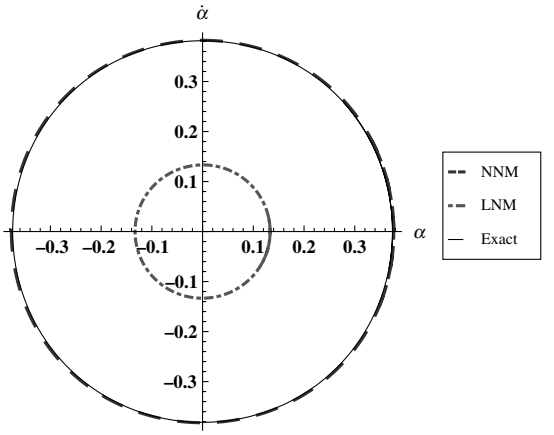

b) Pitch

Fig. 3 LCO phase-space plots of quasi-steady airfoil at $1.05V_f$.

even though they are very, very small. Due to the inexactness of the NNM, which is used to generate the modal initial condition for the simulation of the original equations of motion, an extremely small part of the LCO mode is excited by the initial condition. If the simulation of the exact equations of motion is allowed to run for long enough, the LCO motion will begin to appear. This is shown in Fig. 5. Because this growth is due to inaccuracies in the initial condition, the modal solutions do not show this motion growth.

The results for the NNM are not always as good as in the above example. If the nonlinearities in the system are too strong, the asymptotic NNM will not perform as well. Figure 6 is the same system as above except the nondimensional freestream velocity has been increased to 1.17 times the linear flutter velocity. The higher velocity causes a higher amplitude. This makes the system nonlinearity stronger because the nonlinearity is dependent on the amplitude. In the figure, it is obvious that neither the NNM nor

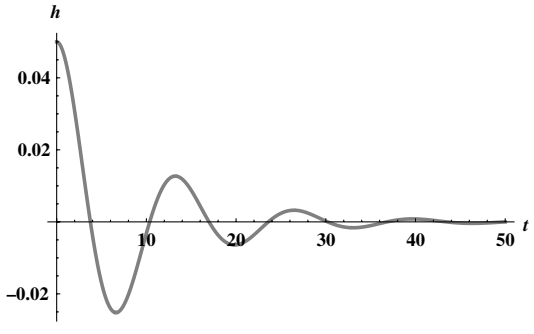

Fig. 4 Damped mode time-history plot of quasi-steady airfoil at $1.05V_f$.

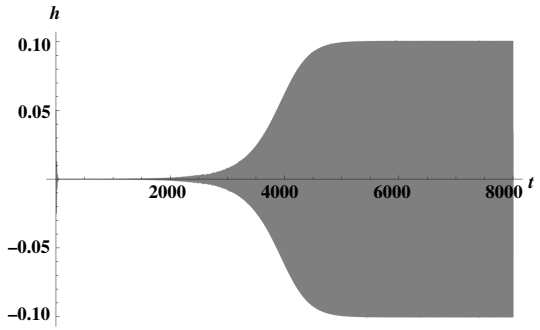

Fig. 5 Growth of LCO motion in exact system due to approximate damped mode initial condition.

the LNM are doing a good job of modeling the exact solution, but the NNM is much better than the LNM. Figures 7 and 8 show the frequencies and amplitudes of LCO as the freestream velocity is increased. These figures also display the degradation of the NNM solution when the velocity is increased. If the velocity is increased further, the asymptotic solution produces a divergent solution even though a LCO still exists for the exact solution.

Typically, one can increase the order of the approximation to improve the results. For the example, increasing the order produces a reasonable convergence for $1.01V_f$. Figure 9 shows the convergence of the solution at $1.05V_f$ as the order of the approximation is increased. The figure demonstrates that an increase in order and computational effort does not guarantee an increase in the accuracy of the solution; however, for the weakly nonlinear system evaluated, the

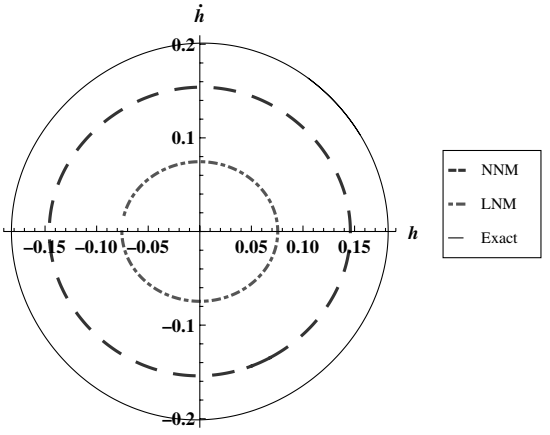

a) Plunge

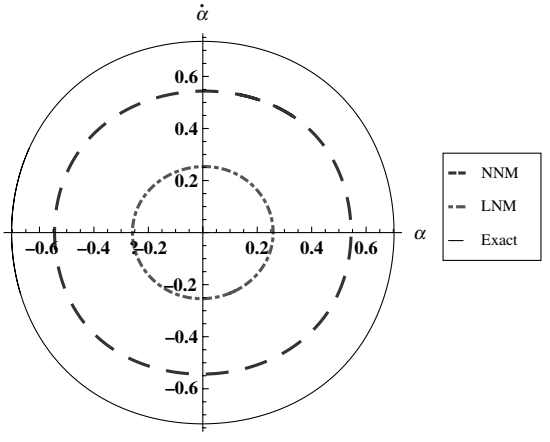

b) Pitch

Fig. 6 LCO phase space plots of quasi-steady airfoil at $1.17V_f$.

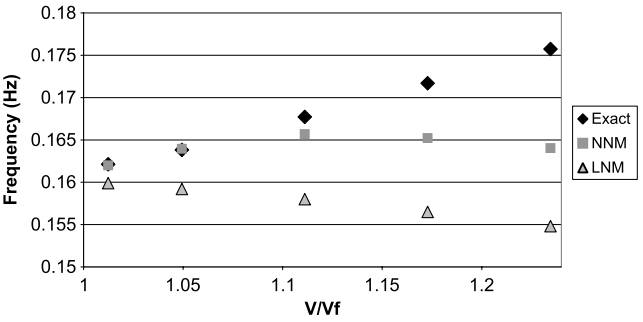

Fig. 7 LCO frequency trend with increasing velocity.

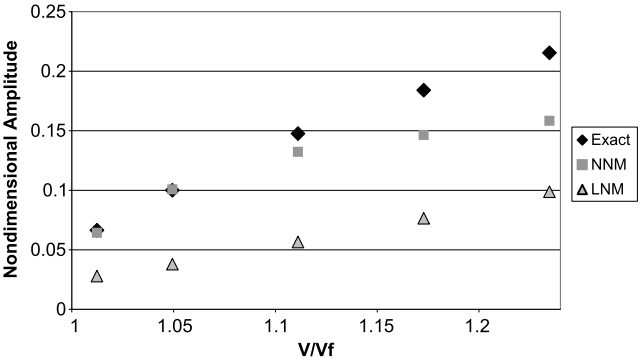

Fig. 8 LCO amplitude trend with increasing velocity.

NNM solution generally converges toward the exact solution as the order is increased. When the velocity is further increased to $1.17V_f$ the convergence becomes more unreliable. The third-order solution is an improvement, but the fifth-order produces an unstable solution. The seventh-order solution is better than the third, but the error again increases with the ninth-order solution. The result was somewhat expected as Shaw and Pierre state in their papers that an increase in the order of approximation is unreliable [13].

C. Master Coordinate Study

Each nonlinear normal mode is built off a specific master coordinate. Because the resulting mode is an approximation, the selection of the master coordinate affects the accuracy of the results. The master coordinate can be directly a degree of freedom or it can be a modal coordinate. Throughout this work, three different master coordinates were used for the pitch-plunge airfoil model. They are referred to as degree of freedom, linear structural modes (with apparent mass), and linear flutter mode. Each is discussed in detail below.

1. Degree of Freedom

The easiest master coordinate to use is one of the degrees of freedom of the system. The aeroelastic system from Eq. (1) was rewritten as

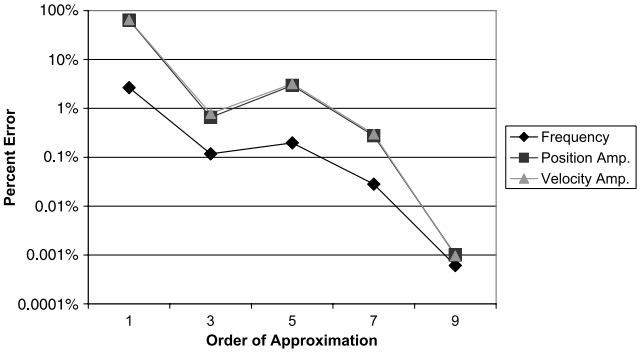

Fig. 9 Asymptotic convergence at $1.05V_f$.

$$[M]\{\ddot{q}_i\} = f_i[\{q_i\}, \{\dot{q}_i\}] \tag{29}$$

Note that the mass matrix $[M]$ above is the aeroelastic mass matrix and thus includes the apparent mass effects from the aerodynamic model. Both sides of the above equation are then multiplied by the inverse of the mass matrix to get

$$\{\ddot{q}_i\} = [M]^{-1} f_i[\{q_i\}, \{\dot{q}_i\}] \tag{30}$$

Now one of the degrees of freedom may be used as the master coordinate. This master coordinate is referred to as the plunge or pitch master coordinate.

2. Linear Structural Mode Shapes with Apparent Mass

The second master coordinate used was the linear structural mode shapes with apparent mass effects. This is a modal degree of freedom used as the master coordinate. To find this modal coordinate, the aeroelastic system in Eq. (1) was linearized and the freestream velocity was set to zero.

$$\begin{pmatrix} 1+\frac{1}{\mu} & x_\alpha - \frac{a}{\mu} \\ x_\alpha - \frac{a}{\mu} & r_\alpha^2 + \frac{1}{8\mu} + \frac{a^2}{\mu} \end{pmatrix} \begin{pmatrix} \ddot{h} \\ \ddot{\alpha} \end{pmatrix} = \begin{pmatrix} 0 & 0 \\ 0 & 0 \end{pmatrix} \begin{pmatrix} \dot{h} \\ \dot{\alpha} \end{pmatrix} - \begin{pmatrix} \bar{\omega}^2 & 0 \\ 0 & r_\alpha^2 \end{pmatrix} \begin{pmatrix} h \\ \alpha \end{pmatrix} \tag{31}$$

A standard linear-modal analysis was preformed and the modal transformation matrix was found. The linear modal transformation matrix was used to transform the nonlinear system. Because the aeroelastic mass matrix is linear and does not depend on the velocity, the transformation converts it to an identity matrix and system will be of the form below.

$$\{\ddot{\eta}_i\} = f_i[\{\eta_i\}, \{\dot{\eta}_i\}] \tag{32}$$

With the nonlinear system written in terms of η_i, each of the modal coordinates could be used as the master coordinate and are referred to as the S. Mode 1 and S. Mode 2 master coordinates.

3. Linear Flutter Mode

The linear flutter mode was also used as a modal master coordinate. Starting with the aeroelastic equations of motion in Eq. (1), the system was linearized. The velocity of interest (above the linear flutter velocity) was chosen and the left and right modal transformation matrices were calculated. When these transformation matrices are applied to a linearized system in first-order form, it results in a block diagonal matrix with submatrices of the form (that may be used to convert to a second-order decoupled form) [21]:

$$\begin{bmatrix} 0 & 1 \\ C_1 & C_2 \end{bmatrix} \tag{33}$$

When these same transformation matrices are applied to the nonlinear first-order system matrix, the resulting matrix is fully populated. Assuming a cubic pitch stiffness nonlinearity, the block diagonal parts take the form seen below and the off-block diagonal terms are constants times α^2 instead of zeros as in the linear case.

$$\begin{bmatrix} C_3\alpha^2 & 1 + C_4\alpha^2 \\ C_1 + C_5\alpha^2 & C_2 + C_6\alpha^2 \end{bmatrix} \tag{34}$$

This first-order system of equations obviously cannot be converted back to second-order form and is consequently not in the form needed for the standard derivation of NNM. Thus, the first-order formulation had to be utilized anytime the linear flutter mode was used as the master coordinate. When choosing the two master coordinates from the first-order system, the two states that would create the flutter mode from the linear matrix must be selected. If the other pair that creates the damped mode is selected, the LCO will not be found.

4. Master Coordinate Results

Figures 10 and 11 show the results from the master coordinate study. Note that the vertical axis is logarithmic. The percent error of the NNM solution is plotted against increasing velocity. The errors are found by comparing the NNM solution to the simulation of the original equations of motion. The percent error was calculated for the frequency, the displacement amplitude of the master and slave coordinates, and the velocity amplitude of the master and slave coordinates. The average of all four amplitude errors gave an integrated picture of how the NNM was performing. The average

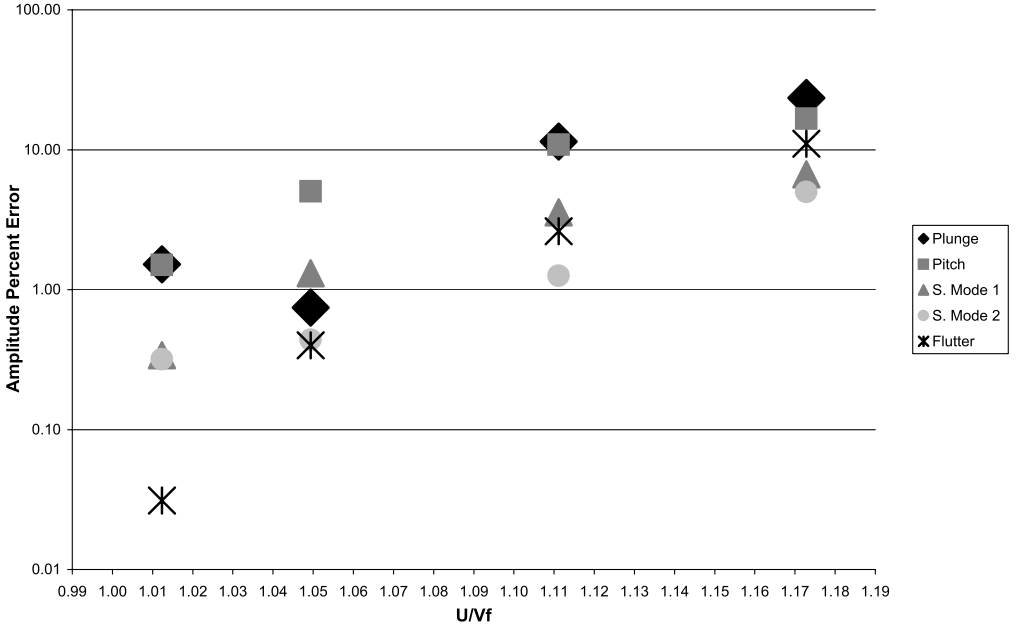

Fig. 10 Master coordinate amplitude error results.

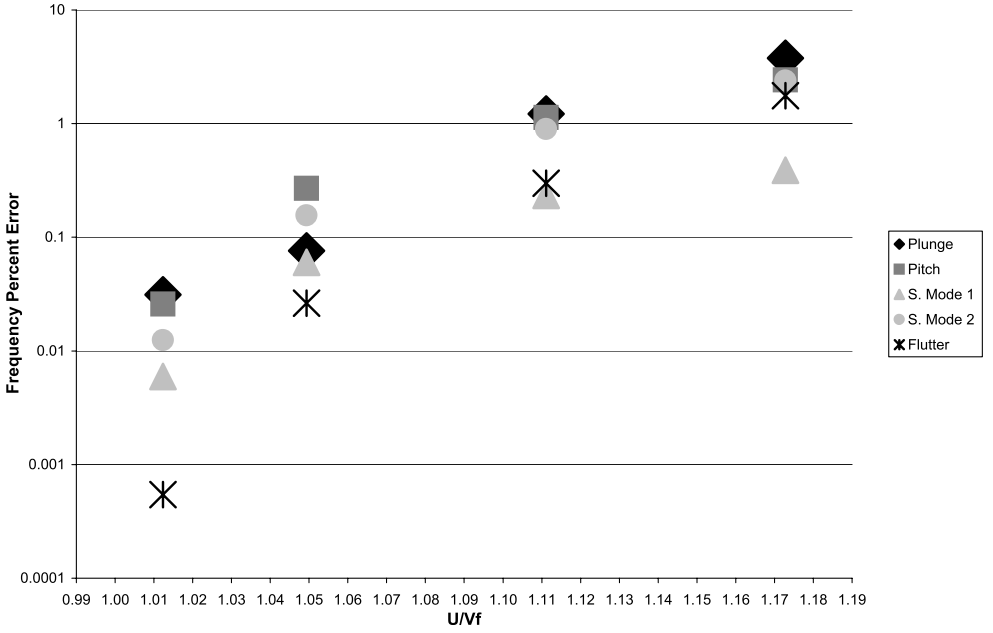

Fig. 11 Master coordinate frequency error results.

amplitude error is presented in Fig. 10. The master coordinates are as described in the preceding paragraphs.

It is obvious from the figures that the accuracy of the results is dependent on the selection of the modal coordinate. It is not immediately apparent what the best coordinate would be. Selection would appear to depend on what velocity was of interest. The results for all of the master coordinates degrade as the velocity increases. This is caused by the larger amplitude LCO at the higher velocities creating a system that effectively has a stronger nonlinearity. Within about 10% of the flutter velocity, the linear flutter mode gives the best results for both amplitude and frequency. After this point, the results using the linear flutter master coordinate are not the best and give a divergent solution at $1.19V_f$ (just beyond the range of the plot). At a certain velocity (or amplitude), all the simulations using NNMs based on an asymptotic formulation will diverge. In this case, the linear flutter master coordinate is the first to diverge. The structural mode shapes are not far behind and produce a divergent solution at $1.29V_f$. The pitch and plunge master coordinates produce an LCO much longer (approximately $2V_f$), but as can be seen in the error plots, they have a large error even at $1.17V_f$. Because the flutter mode is the most accurate in the low-velocity range where the asymptotic method can be trusted, it is the best master coordinate.

D. Pitch-Plunge Airfoil with Unsteady Aerodynamics

Results are presented for the unsteady aerodynamics case in this section. The model parameters are the same as the quasi-steady case presented earlier. The dimensionless linear flutter velocity for this system is 1.699 and the linear flutter frequency is 0.1387 Hz. The linear flutter mode was selected as the master coordinate for this test case. As previously discussed in the master coordinate section, the two first-order modal degrees of freedom that correspond to the linear flutter mode must be selected. If the first-order degrees of freedom corresponding to the damped linear mode (or those corresponding to the aerodynamic states) are selected, the LCO will not be found. Instead, only the damped motion will be found. With the linear flutter mode as the master coordinate, a single NNM is found. If another master coordinate were used, pitch for instance, there would be three solutions to the linear modal coordinates. With the corresponding nonlinear coefficient solutions, these would create two meaningful NNMs corresponding to the LCO mode and the damped mode. The third is an aerodynamic lag mode. The use of the linear flutter mode simplifies the process and results.

The final result of using the linear flutter mode on the unsteady aeroelastic system is a single set of coupled first-order equations.

$$\begin{aligned}\dot{u} = {} & u(0.0769 + 0.00524u^2 + 0.1301v^2 - 0.001716u^4 \\ & + 0.0241u^2v^2 + 0.0455v^4 + 0.0001875u^6 - 0.001861u^4v^2 \\ & + 0.00566u^2v^4 + 0.00530v^6 - 6.83\times10^{-6}u^8 - 0.000254u^6v^2 \\ & - 0.0001571u^4v^4 + 0.000340u^2v^6 + 0.000205v^8) \\ & + v(-0.728 - 0.0452u^2 - 0.1247v^2 + 0.00357u^4 \\ & - 0.0686u^2v^2 - 0.0421v^4 + 0.000840u^6 - 0.00653u^4v^2 \\ & - 0.01373u^2v^4 - 0.00474v^6 - 0.0000754u^8 - 0.000229u^6v^2 \\ & - 0.000781u^4v^4 - 0.000741u^2v^6 - 0.0001777v^8) \end{aligned} \tag{35}$$

$$\begin{aligned}\dot{v} = {} & u(0.728 + 0.00844u^2 + 0.210v^2 - 0.00277u^4 + 0.0388u^2v^2 \\ & + 0.0733v^4 + 0.000302u^6 - 0.00230u^4v^2 + 0.00913u^2v^4 \\ & + 0.00854v^6 - 0.00001101u^8 - 0.000409u^6v^2 \\ & - 0.000253u^4v^4 + 0.000548u^2v^6 + 0.000331v^8) \\ & + v(0.0769 - 0.0729u^2 - 0.201v^2 + 0.00575u^4 - 0.1106u^2v^2 \\ & - 0.0679v^4 + 0.001354u^6 - 0.01053u^4v^2 - 0.0221u^2v^4 \\ & - 0.00764v^6 - 0.0001215u^8 - 0.000368u^6v^2 - 0.001259u^4v^4 \\ & - 0.001194u^2v^6 - 0.000287v^8) \end{aligned} \tag{36}$$

The Runge-Kutta simulation of these equations is compared to linear normal mode equations and the exact equations in Figs. 12 and 13. The figures represent the results at a freestream velocity of 1.05 and 1.17 times the linear flutter velocity, respectively. As with the quasi-steady results, the NNM works well at lower amplitudes and the error increases with amplitude. The NNM always performs better than the LNM just as in the quasi-steady cases. As can be seen, especially in the higher velocity case, the phase-space plot shape for the unsteady aerodynamics is very different from in the quasi-steady aerodynamic cases. This difference in the nature of the motion is also captured by the NNM solution.

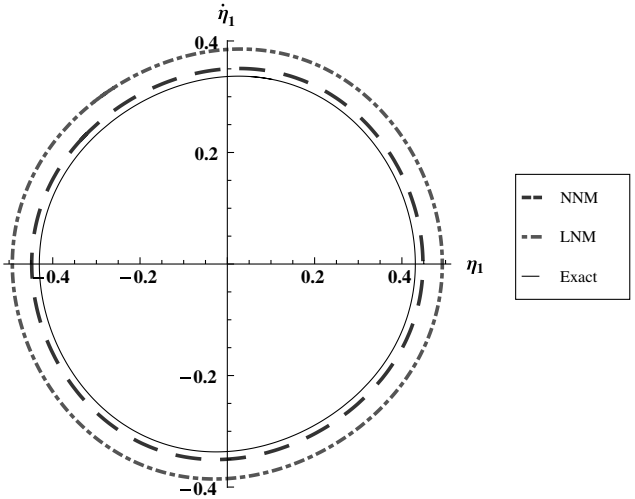

Fig. 12 LCO phase space results at $\bar{U} = 1.05V_f$, unsteady aerodynamics.

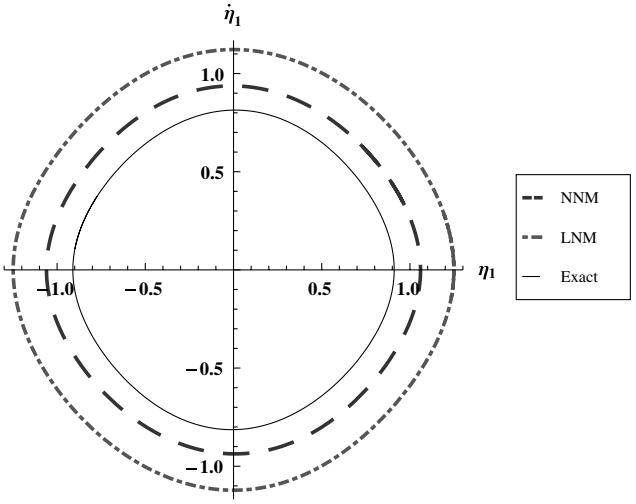

Fig. 13 LCO phase space results at $\bar{U} = 1.17V_f$, unsteady aerodynamics.

IV. Conclusions

Nonlinear aeroelastic systems exhibiting limit cycle oscillations were successfully modeled using nonlinear normal modes. A first-order version of the NNM method was formulated to allow the use of unsteady aerodynamics and the use of the linear flutter mode as a master coordinate. The asymptotic method of approximation was shown to be sufficient for velocities slightly in excess of the linear flutter velocity, but the error increased with large amplitudes at higher velocities due to the increased strength of the nonlinearity. The asymptotic method does not necessarily converge with each increase in the order of the approximation. The master coordinate used to construct the nonlinear normal mode was shown to have a significant effect on the accuracy of the simulation and the linear flutter mode was identified as best choice because it produced a more accurate solution and solving for the unknown coefficients was easier.

Based on the results in this paper, the nonlinear normal mode method appears to be a good option to help analyze limit cycle oscillation in aeroelastic systems. With the proper selection of master coordinates, the semi-analytic nature of the method offers valuable insight into the mechanism of the motion. Further work in coefficient solution techniques is necessary to reliably improve the accuracy of the solution and apply nonlinear normal modes to practical applications involving systems with a large number of degrees of freedom.

References

[1] Bunton, R. W., and Denegri, C. M. Jr., "Limit Cycle Oscillation Characteristics of Fighter Aircraft," *Journal of Aircraft*, Vol. 37, No. 5, 2000, pp. 916–918. doi:10.2514/2.2690

[2] Denegri, C. M. Jr., "Limit Cycle Oscillation Flight Test Results of a Fighter with External Stores," *Journal of Aircraft*, Vol. 37, No. 5, 2000, pp. 761–769. doi:10.2514/2.2696

[3] Denegri, C. M. Jr., , Dubben, J. A., and Maxwell, D. L., "In-Flight Wing Deformation Characteristics During Limit-Cycle Oscillations," *Journal of Aircraft*, Vol. 42, No. 2, 2005, pp. 500–508. doi:10.2514/1.1345

[4] Dowell, E., Thomas, J., Hall, K., and Denegri, C. J., "Theoretical Predictions of F-16 Fighter Limit Cycle Oscillations for Flight Flutter Testing," *Journal of Aircraft*, Vol. 46, No. 5, 2009, pp. 1667–1672. doi:10.2514/1.42352

[5] Woolston, D., Runyan, H., and Byrdsong, T., "Some Effects of System Nonlinearities in the Problem of Aircraft Flutter," TR, NACA TN-3539, 1955.

[6] Lee, B., and LeBlanc, P., "Flutter Analysis of a Two-Dimensional Airfoil with Cubic Nonlinear Restoring Force," TR, National Research Council of Canada, Aeronautical Note, NAE-AN-36, NRC No. 25438, 1986.

[7] Houbolt, J., "A Recurrence Matrix Solution for the Dynamic Response of Elastic Aircraft," National Research Council of Canada NAE-AN-36, NRC No. 25438, 1959.

[8] Price, S. J., Alighanbary, H., and Lee, B. H. K., "The Aeroelastic Response of a Two-Dimensional Airfoil with Bilinear and Cubic Structural Nonlinearities," *Journal of Fluids and Structures*, Vol. 9, No. 2, Feb. 1995, pp. 175–193. doi:10.1006/jfls.1995.1009

[9] Krylov, N., and Bogoliubov, N., *Introduction to Nonlinear Mechanics, translation by Solomon Lifschitz*, Princeton Univ. Press, Princeton, New Jersey, 1947.

[10] Lee, B., Gong, L., and Wong, Y., "Analysis and Computation of Nonlinear Dynamic Response of a Two-Degree-of-Freedom System and its Application in Aeroelasticity," *Journal of Fluids and Structures*, Vol. 11, No. 3, 1997, pp. 225–246. doi:10.1006/jfls.1996.0075

[11] Liu, L., Wong, Y., and Lee, B., "Application of the Centre Manifold Theory in Non-Linear Aeroelasticity," *Journal of Sound and Vibration*, Vol. 234, No. 4, 2000, pp. 641–659. doi:10.1006/jsvi.1999.2895

[12] Kerschen, G., Peeters, M., Golinval, J., and Vakakis, A., "Nonlinear Mormal modes, Part I: A useful framework for the structural dynamicist," *Mechanical Systems and Signal Processing*, Vol. 23, No. 1, 2009, pp. 170–194. doi:10.1016/j.ymssp.2008.04.002

[13] Shaw, S., and Pierre, C., "Normal Modes for Non-Linear Vibratory Systems," *Journal of Sound and Vibration*, Vol. 164 No. 1, 1993, pp. 85–124. doi:10.1006/jsvi.1993.1198

[14] Shaw, S., and Pierre, C., "Normal Modes of Vibration for Non-Linear Continuous Systems," *Journal of Sound and Vibration*, Vol. 169, No. 3, 1994, pp. 319–347. doi:10.1006/jsvi.1994.1021

[15] Pesheck, E., Boivin, N., Pierre, C., and Shaw, S., "Nonlinear Modal Analysis of Structural Systems Using Multi-Mode Invariant Manifolds," *Nonlinear Dynamics*, Vol. 25, Nos. 1–3, 2001, pp. 183–205. doi:10.1023/A:1012910918498

[16] Pesheck, E., Pierre, C., and Shaw, S., "A New Galerkin-Based Approach for Accurate Non-Linear Normal Modes Through Invariant Manifolds," *Journal of Sound and Vibration*, Vol. 249 No. 5, 2002, pp. 971–993. doi:10.1006/jsvi.2001.3914

[17] Jiang, D., Pierre, C., and Shaw, S., "Nonlinear Normal Modes for Vibratory Systems Under Harmonic Excitation," *Journal of Sound and Vibration*, Vol. 288, Nos. 4–5, 2005, pp. 791–812. doi:10.1016/j.jsv.2005.01.009

[18] Bisplinghoff, R., Ashley, H., and Halfman, R., *Aeroelasticity*, Addison Wesley Longman, Reading, MA, 1955.

[19] Theodorsen, T., "General Theory of Aerodynamic Instability and the Mechanism of Flutter," TR, NACA, Rept. 496, 1935.

[20] Venkatesan, C., and Friedmann, P., "New Approach to Finite-State Modeling of Unsteady Aerodynamics," *AIAA Journal*, Vol. 24, No. 12, 1986, pp. 1889–1897. doi:10.2514/3.9545

[21] Patil, M. J., "Decoupled Second-Order Equations and Modal Analysis of a General Nonconservative System," In *Proceedings of the AIAA Dynamics Specialists Conference*, Atlanta, Georgia, AIAA, Reston, VA, 2000; also AIAA Paper 2000-1654.